

# Oort Cloud Bombardment by Dark Matter

Jeremy Mould

Swinburne University; jmould@swin.edu.au

ARC Centre of Excellence for Dark Matter Particle Physics

## Abstract

The realization that primordial black holes (PBHs) might be some fraction of the dark matter begged the question, how often do PBHs enter the solar system? For a Neptune radius solar system the answer is, rarely. For an Oort cloud sized system the answer is different. Simulations of bombardment of the Oort cloud by dark matter suggest that dislodgement of protocomets and their entry into the inner solar system can match the observed frequency of comets, if that PBH fraction is high enough. Comets were traditionally considered as messengers, usually omens. After 50 years of puzzlement regarding dark matter, we need a hint from the dark universe about the size and nature of dark matter particles.

## 0 Introduction

Besides nearby planets, comets were the first recorded periodic astronomical phenomena. Could they also be telling us about the first component of our Galaxy to form, its dark halo? The tidal force from the Galactic disk is believed to be the dominant external force in the evolution of the bodies in the Oort cloud (Dones et al. 2004). The vertical component (i.e., perpendicular to the Galactic plane) of the Galactic tide is thought to play the most important role in the formation of the Oort cloud and the production of long-period comets from it (e.g., Harrington 1985, Heisler & Tremaine 1986), but a radial component is also included by Higuchi (2007). Collins & Sari (2010) note that both passing stars and tidal torques are factors to be taken into account.

This may not be the only force impinging on the Oort cloud, however. If dark matter consists of macroscopic particles as opposed to WIMPs (Weakly Interacting Massive Particles) or axions, the effects may be observable in the form of comets. Here we focus on lunar mass particles, nominally  $10^{-7} M_{\odot}$ . These might be primordial black holes (PBH, Murai, Sakurai & Takahashi 2025); they might be axion miniclusters (Fairbairn et al. 2025), or they might be free floating moons (FFM). Microlensing experiments are unable to tell the difference (Kühnel 2025). Here one can be agnostic as to which dark matter (DM) particles form the local density of  $0.01 M_{\odot} \text{ pc}^{-3}$ . But it should be noted that it is not tenable that the rest of the DM in the universe is FFMs, as they are baryonic, and the baryonic fraction of matter is 0.0224/0.12 ( Planck collaboration 2020). Like other DM candidates, both PBHs and FFMs lack an understanding of the exact formation mechanism.

Other signs of DM activity in the solar system have been suggested. De Rocco (2025) notes that DM in the form of macroscopic composites is largely

unconstrained at masses of  $10^{11} - 10^{17}$  g. In this mass range, DM may collide with planetary bodies, depositing energy and leaving dramatic surface features that remain detectable on geological timescales. He suggests that Ganymede, the largest Jovian moon, provides a prime target to search for DM impacts due to its differentiated composition and Gyr-old surface. There are also searches for microscopic dark matter, such as WIMP capture in the Sun. Stothers (1984) was first to connect DM and comets, after the appearance of heavy halo models of the Galaxy (e.g. Caldwell & Ostriker 1981).

The collision rate for objects incident on the solar system is  $\sigma v n$ , where  $\sigma$  is the geometric cross section for the solar system,  $v$  is their velocity and  $n$  is their number density. The ratio of dark matter rate to stellar rate is  $n_{DM}/n_* v_{DM}/v_*$  which equals  $\rho_{DM}/m_{DM} v_{DM}$  divided by  $\rho_*/m_* v_*$ , where  $\rho$  is density and  $m$  is mass. For  $m_{DM} = 10^{-7} M_\odot$ , the rate ratio is  $10^7 0.01/0.1 220/30$  for old disk stars that dominate the solar neighbourhood. So the DM bombardment rate is ten million times larger than the stellar rate. In fact, the conventional theory is not that stars perturb the Oort cloud. It is that the tidal field of the Galaxy perturbs the Oort cloud.

The nature of the DM remains one of the outstanding questions of 21st century astrophysics. Microlensing observations with the Rubin telescope could be prioritized to discover subsolar mass objects (Romao, Croon & Godines 2025). Strong limits on fundamental particle DM are being set by physicists (Aalbers et al. 2023, Barberio et al. 2025). These may nevertheless be an important component of the DM, but they do not dislodge protocomets.

In the next section a toy model is developed to examine the effectiveness of lunar mass DM. In §2 results of these simulations are presented. They are discussed in §3. The conclusion is that within the mass range discussed macroscopic DM is a plausible contributor to the rate of comet production.

## 1 A toy model

The cumulative number of protocomets in the Oort cloud is given as  $N \propto D^{-\alpha}$ , for  $D \sim 2.8$  km, with  $\alpha = 3.6$  for larger  $D > 2.8$ , and  $\alpha = 0.5$  for smaller objects (Wajer et al. 2024). The Oort cloud contains  $\sim 3.8 \times 10^8$  comets with  $D > 10$  km (Nesvorný 2018). Extending this to decimeter size (Vida et al. 2023) we obtain  $N = 1.5 \times 10^{14}$ , compared with  $10^{12} - 10^{13}$  (Wiegert & Tremaine 1998). The Oort cloud is taken to be spherical, which is appropriate to its outer parts. The number of comets in the simulation is 250,000, compared with our adopted  $N = 4 \times 10^{13}$  and so the fraction of  $4\pi$  sr in the simulation is given by  $\pi\theta^2/4\pi = 2.5 \times 10^5/N$ , where  $\theta$  is the half angle.

The adopted distribution radius  $r$  from the sun is (Dehnen 1993) a number density of

$$n \propto \frac{a}{r^2(r+a)^2} \quad (1)$$

where  $a = 10^5$  AU and the rate of intrusion by lunar mass objects can be calculated from the number density and the object velocity, taken to be, without

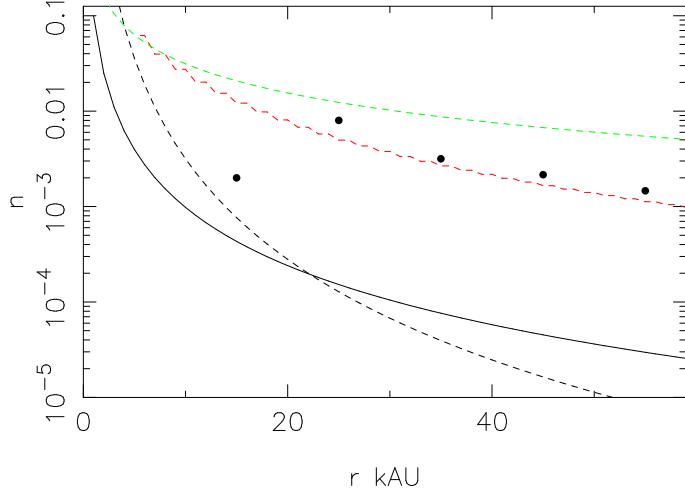


Figure 1: The Dehnen (1993) distribution in the solid line. Other authors suggest a radial power law with index -3.5, and this is shown by the dashed line. Brasser et al. (2006) finds that the median distance falls off as  $\sqrt{n}$ . Two variants of this density law are shown as the red and green dashed lines respectively. The distribution adopted by Kaib & Quinn (2008) is represented by the solid symbols, based on the cumulative distribution they provide.

loss of generality, in the  $yz$  plane, where  $z$  is the axis from the Sun at the origin to the Oort Cloud protocomet. Intercometary forces are neglected, again without much loss of generality. Distributions by Duncan et al. (1987) and Dones et al. (2004) are compared in Figure 1. Kaib et al. (2011) note that the radius of the Oort cloud,  $a$ , may have varied over time with the migration of the Sun in its radial distance from the Galactic Centre. There are other density distributions in the literature and these are compared in Figure 1. The velocity distribution of the perturbers has two components, that due to the Sun's galactic orbit,  $220 \text{ km s}^{-1}$  in the  $yz$  plane and the galactic halo's  $110 \text{ km s}^{-1}$  velocity dispersion with an isotropic distribution. Solar system units are adopted with  $M = v_{30}^2 r$  with masses in solar units,  $v_{30}$  in Earth orbital velocity units,  $r$  in AU, and  $G = 1$ .

The impact parameter,  $b$ , of the incoming object is a crucial parameter. I assume this lies with uniform probability within a sphere of radius  $b_{max} \approx M \text{ AU}$ , where  $M$  is the mass of the object in  $M_\odot$  units. For an impact velocity,  $v$ , this gives a momentum transfer, when the interaction with the protocomet is complete, of,

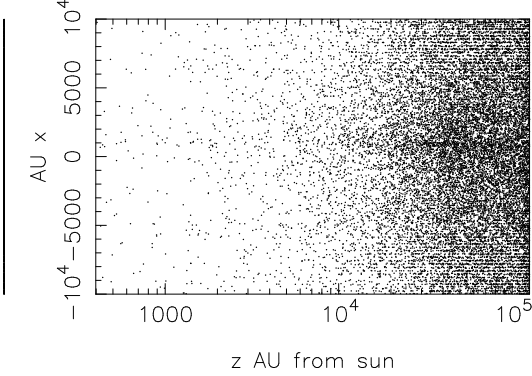


Figure 2: Distribution of particles in the xz plane 0.05 Myrs into run 25.

$$\Delta p = 2GMm/bv \quad (2)$$

with  $m$  the mass of the perturbed particle, whose velocity is parallel to the vector from its original position to the impact parameter position. We then follow the orbits of 250,000 such particles with time intervals of 0.10 to 0.3 yr. The integration scheme was simply  $\delta\mathbf{v} = \mathbf{a} dt$ , where  $\mathbf{a}$  is the acceleration, followed by  $\delta\mathbf{r} = \mathbf{v} dt$ , where  $\mathbf{v}$  is the velocity. Simulations with different DM masses and other parameters are recorded in Table 1. Any protocomet reaching the inner solar system with radius 300 AU is noted. This choice of radius is on the large size, but the simulations are limited by small number statistics, and a markedly smaller radius would be prohibitive in computer time and not necessary for this first exploration of the hypothesis.

With these initial conditions we are neglecting the perturbers that arrive with impact parameters larger than  $b_{max}$ , and also oversupplying impacts by a factor  $4(a/b_{max})^2/N$ , where  $N$  is the number of protocomets in the Oort cloud. The arrival rate of DM particles at the Oort cloud<sup>1</sup> is  $rate_1 \approx 4\pi\rho a^2 v/m$ , where  $\rho$  is the local density of DM,  $0.01 M_\odot pc^{-3}$  (de Salas & Widmark 2021) and  $v$  is the solar velocity of  $220 \text{ km s}^{-1}$  (Binney 2011).

There are two factors for which the simulation comet finding rate needs to be corrected, (1) the lost area factor in which DM particles falling outside the maximum adopted impact parameter are neglected ( $4 a^2/b_{max}^2 / N$ ) and (2) the number of protocomets in the simulation, compared with  $N$ . With these

<sup>1</sup> As a spherical shell the DM traverses it both on the windward and the leeward side. There is also a DM velocity dispersion of  $110 \text{ km s}^{-1}$  (Freeman 1985).

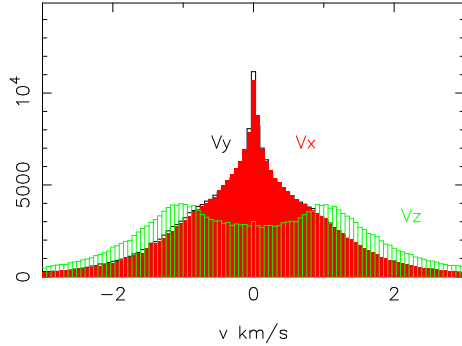


Figure 3: Distribution of velocities 0.05 Myrs into run 25.

corrections the predicted rate of entry of comets into the inner solar system<sup>2</sup> is

$$\text{rate}_2 = \frac{\text{rate}_1}{4} \frac{\Delta t}{a^2} \frac{N^2}{2.5 \times 10^5} \frac{b_{max}^2}{\Delta t} n = 1.6 \times 10^{-3} n b_7^2 \text{rate}_1, \quad (3)$$

where  $n$  is the number recorded in the simulation in time  $\Delta t$ , and  $b_7 = b_{max} \times 10^7$ . Figures 2 & 3 show the particle distribution and their velocity distribution shortly after the start of a simulation.

## 1.1 Results

Figure 5 shows  $\text{rate}_2$  for a range of DM masses and maximum impact parameters, assuming that all the DM has mass  $M$ , i.e.  $f_{PBH} = 1$  in the case of PBH. The comet arrival rate in the inner solar system  $\text{rate}_2 > 10$  per year for some maximum impact parameter for  $10^{-9} < M < 10^{-5} M_\odot$ . The rate would be brought down to order unity for  $f_{PBH} = 0.1$ . The shallower Oort cloud distributions shown in Figure 1 would be expected to reduce the comet rate proportionally to the median radius. This was borne out in re-runs of # 19 and 20 with an  $r^{-3.5}$  density dependence.

## 2 Comet supply and demand

An equally fraught extrapolation to equation (3) in the present work is the estimation of the number of comets inside 300 AU from the known number

---

<sup>2</sup>The Oort cloud is generally considered a spherical or almost spherical region, but it also has an inner, disc-shaped component that is more aligned with the ecliptic plane (the plane of the solar system). The outer Oort cloud is a vast, spherical halo extending far beyond the Kuiper Belt, while the inner Oort cloud is thought to be more of a donut shape and closer to the ecliptic.

Table 1: Simulations

run #	M M <sub>⊕</sub>	b <sub>max</sub> AU	n	Δt Myrs	max v km s <sup>-1</sup>	<ε>	Nb <sub>7</sub> /a	rate <sub>1</sub> yr <sup>-1</sup>	rate <sub>2</sub> yr <sup>-1</sup>
19	10 <sup>-9</sup>	10 <sup>-7</sup>	20	31.5	1.5	0.5	4000	62	2.0
20	10 <sup>-8</sup>	10 <sup>-7</sup>	7	5.5	3.4	0.7	4000	6.2	0.07
21	10 <sup>-7</sup>	10 <sup>-6</sup>	7	3.7	2.5	0.7	40000	0.62	7
22	10 <sup>-8</sup>	10 <sup>-6</sup>	20	28.1	1.6	0.74	40000	6.2	20
23	10 <sup>-9</sup>	10 <sup>-6</sup>	2	18.1	1.4	1.14	40000	62	20
24	10 <sup>-9</sup>	10 <sup>-6</sup>	0	18.1	—	—	40000	62	0
25	10 <sup>-6</sup>	10 <sup>-6</sup>	41	1.8	80.4	1.0	40000	0.062	0.41
26	10 <sup>-9</sup>	10 <sup>-8</sup>	7	5.2	4.5	0.79	400	62	0.07
27	10 <sup>-8</sup>	10 <sup>-8</sup>	16	5.2	45.2	1.62	400	6.2	0.016
28	10 <sup>-10</sup>	10 <sup>-8</sup>	2	5.5	1.8	0.62	400	616	0.2
29	10 <sup>-7</sup>	10 <sup>-8</sup>	25	0.4	88.5	0.91	400	0.62	0.00025
30	10 <sup>-10</sup>	10 <sup>-9</sup>	3	18.9	2.0	0.74	40	616	1.5×10 <sup>-5</sup>
31	10 <sup>-10</sup>	10 <sup>-7</sup>	0	4.1	—	—	40	616	0
32	10 <sup>-6</sup>	10 <sup>-5</sup>	3	16.1	1.9	0.64	4×10 <sup>5</sup>	0.062	3
33	10 <sup>-7</sup>	10 <sup>-5</sup>	2	8.1	4.3	2.2	4×10 <sup>5</sup>	0.62	20
34	10 <sup>-8</sup>	10 <sup>-5</sup>	0	16.9	—	—	4×10 <sup>5</sup>	6.2	0
35	10 <sup>-5</sup>	10 <sup>-5</sup>	43	4.5	52.3	1.2	4×10 <sup>5</sup>	6.2×10 <sup>-3</sup>	4.3

ε is the ratio of |radial| to tangential velocities; velocities are heliocentric.

rate<sub>1</sub> is PBH arrival; rate<sub>2</sub> is comet entry to the inner solar system.

inside 10 AU. The infall equation in the gravitational field is

$$dr/dt = (1/a - 1/r)^{1/2} = -1/r^{1/2} \quad \text{for small } r \quad (4)$$

for which, after integration, the steady state radial distribution in spherical symmetry is enclosed number n ∼ r<sup>3/2</sup>.

Figure 4 from the JPL small bodies database<sup>3</sup> shows n = 500 inside 10 AU; so n ≈ 82,000 inside 300 AU. With the rate found in the previous section, this can be furnished in a fraction of an Myr. But we need to consider the attrition rate.

---

<sup>3</sup><https://ssd.jpl.nasa.gov>

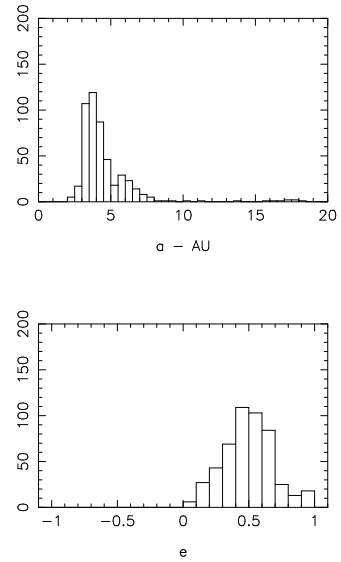


Figure 4: (a) Numbered comet semi-major axes from the JPL small bodies database (above). Orbital eccentricities (below).

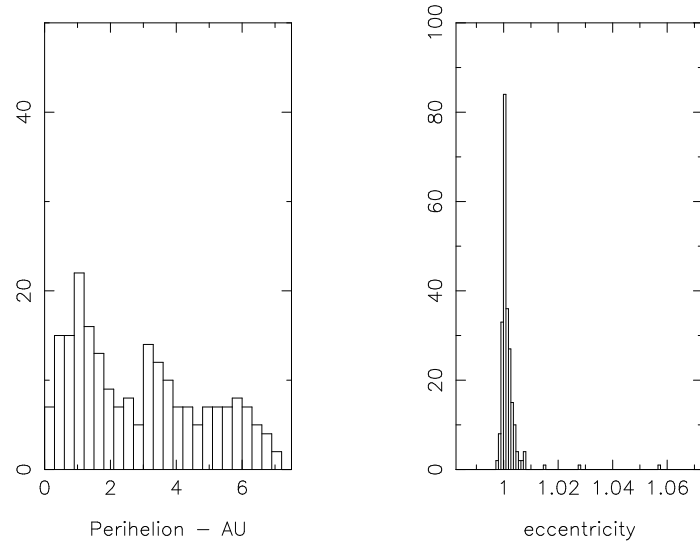


Figure 4: (b) Perihelia and orbital eccentricities from Krolikowska & Dybczynski (2020).

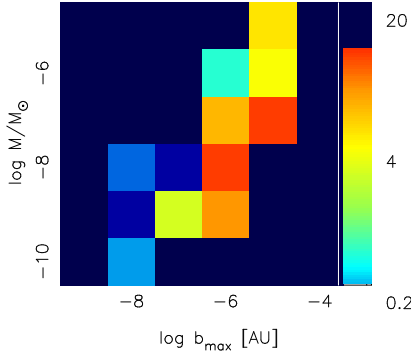


Figure 5: Simulated comet arrival rate in the inner solar system as a function of DM mass and maximum impact parameter. On the right is the colour scale which is logarithmic and ranges from 0.2 to 20. Deeper blue  $< 0.1$ .

The COSINE project (Kwon et al. 2025) used NASA’s WISE and NEO-WISE mission to study 484 comets over 15 years. Of these 68 were on hyperbolic orbits (HC) and 140 were on near parabolic (NPC) orbits . If this sample is typical of our 300 AU volume, and if we consider only the attrition from HCs, the rate is 1.5 per year. If we add in, say, half the NPCs, the rate is double that, which might be hard to sustain for  $f_{PBH} < 0.1$ .

### 3 Discussion

Measuring the fraction of the DM within the mass range we have trialled here that is  $PBH + FFM$  is well within the capabilities of the Rubin and *Roman* telescopes. The optimum microlensing strategy is high cadence and moderate field. This is radically different from that adopted in Rubin’s LSST (Large Survey of Space & Time), which is hemispheric and low cadence. If it is important to the stability of the Oort cloud, or for more general reasons, a special DM survey might be commissioned (see Appendix). The cadence of *Roman* is still being designed, but its aperture  $\times$  field- of-view is 375 times less than Rubin’s. Microlensing has its limitations, of course, dilution by finite source effects and wave optics. These affect the limiting mass detectable,  $\sim 10^{-11} M_\odot$ . Moving to the ultraviolet can gain back a factor of 2; the source star counts contain more main sequence stars and the wave optics less of an issue.

The toy model presented here has looked into one or two of the parameters affecting the arrival of comets in the region of the solar system where we can observe them. A further key parameter is comet mass dispersion. More sophisticated models exist (Bailey 1996), and these could be adapted to further

explore dark matter's involvement with comets. The sculpting of comets by the giant planets is an important factor omitted here.

It should be noted that  $b_{max}$  is, properly speaking, a gratuitous parameter. In a computing world where one could launch billions of particles into orbit from the Oort cloud, it would not be necessary to neglect incoming macroscopic dark matter with large impact parameter; they could be calculated explicitly. Future work should include not only major planets, but also asymptotically large values of  $b_{max}$ , or a maximum impact parameter equal to the mean separation between protocomets in the Oort cloud.

## 4 Conclusions

Depending on the fraction of DM that is of roughly lunar mass, DM may partially (or perhaps, negligibly) contribute to the arrival of comets in the inner solar system. If  $\sim 10\%$  of the DM is PBHs, not only may DM be responsible for forming our Galaxy, but also DM (or FFM), may have had a role (Biver et al. 2024) in forming our water world, a key requirement for life.

## References

Aalbers, J. et al. 2023, JPhG, 50, 3001  
 Alcock, C. et al. 1993, Nature, 365, 621  
 Bailey, M. 1996, EM&P, 57, 72  
 Barberio, E. et al. 2025, JInst, 20, 4001  
 Binney, J. 2011, Prama, 77, 39  
 Binney, J. & Vasiliev, E. 2023 MNRAS, 520, 1832  
 Biver, N., Dello Russo, N. , Opitom, C. & Rubin, M. 2024, *Comets III*, Ed. Karen Meech et al. Space Science Series, UA Press, pp. 459-498  
 Brasser, R., Duncan, M. & Levison, H. 2006, Icarus, 184, 59  
 Caldwell, J. & Ostriker, J. 1981, ApJ, 251, 61  
 De Rocco, W. 2025, PRD, 112, 5023  
 de Salas, P. & Widmark, A. 2021, RPP, 84, 4901  
 Dehnen W., 1993, MNRAS, 265, 250  
 Dones, L., Weissman, P., Levison, H. & Duncan, M. 2004, in *Comets II*, eds. M. Feston, H. Keller & H. Weaver (Tucson: UA Press), p.153  
 Duncan, M., Quinn, T. & Tremaine, S. 1987, AJ, 94, 1330  
 Fairbairn, M., Marsh, D. & Quevillon, J. 1996, PRL, 119, 021101  
 Freeman, K. 1985, IAUS, 106, 113  
 Harrington, R. 1985, Icarus, 61, 60  
 Heisler, J. & Tremaine, S. 1986, Icarus, 65, 13  
 Higuchi, A., Kokubo, E., Kinoshita, H. & Mukai, T. 2007, AJ, 134, 1693  
 Kaib, N. & Quinn, T. 2008, Icarus, 197, 221  
 Kaib, N., Roskar, . & Quinn, T. 2011, Icarus, 215, 491  
 Krolikowska, M. & Dybczynski, P. 2020, A&A, 640, 97

Kühnel, F. 2025, "Positive Indications for Primordial Black Holes", *Primordial Black Holes*, ed Christian Byrnes, Springer, p.453

Kwon, Y. et al. 2025, ApJS, 280, 67

Lepine, J. & Ortiz, R. 1994, A&A, 279, 90

Murai, K., Sakurai, K. & Takahashi, F. 2025, JHEP, 7, 65,

Nesvorný D. 2018, ARAA, 56, 137

Planck collaboration 2020, A&A, 641, A6

Romao, M., Croon, D., Crossey, B. & Godines, D. 2025, MNRAS, 543, 351

Stothers, R. 1984, Nature, 311, 17

Vida, D. et al. 2023, Nat As, 7, 318

Wajer, P. et al. 2024, Icarus, 415, 116065

## Declarations

- Funding: I acknowledge ARC grant CE200100008 which, together with the five Australian university nodes, funds Centre for Dark Matter Particle Physics research.
- Data availability: Data are available from the author.
- Code availability The code comet6.f is available on github: [github.com/jrmould/darkmatter](https://github.com/jrmould/darkmatter), together with a README file.

## Appendix

The PINGAS Galactic star count model (Lepine & Ortiz 1994) without obscuration, together with the Binney & Vasiliev (2023) mass model of the Galaxy, was used to predict the microlensing event rate under the assumption that all the DM was lunar mass PBHs and the simplifying assumption that stars more distant than the Galactic centre were sources. Figure A1 is the result. An optimum cadence for microlensing was assumed, e.g. time before return-to-field = 15 minutes. The comparison with Figure 5 of Romao et al. (2025) (LSST's actual cadence) is informative.

## Acknowledgements

Figure 3 is based on JPL's small bodies database, sponsored by NASA under Contract NAS7-030010. JPL is operated by Caltech for NASA. I acknowledge use of the Swinburne University's Ozstar & Ngarrgu Tindebeek supercomputers, the latter named by Wurundjeri elders and translating as "Knowledge of the Void" in the local Woiwurrung language. I thank colleagues in our microlensing team and the CDMPP for helpful discussions and the referees for improvements to the paper. The PINGAS star counts code is at <http://www.astro.iag.usp.br/~jacques/pingas.html>.

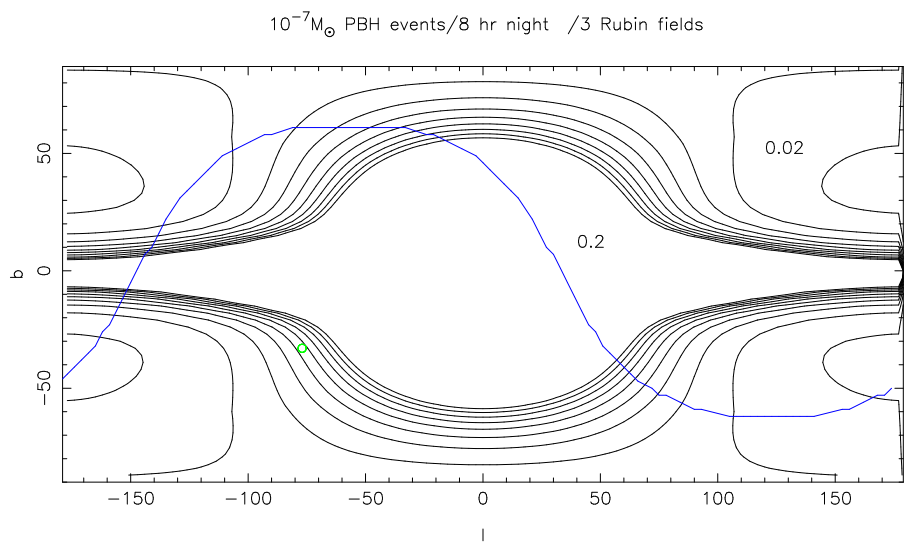


Figure A1: Microlensing event rate per 8 hour night for 3 Rubin fields for 100% lunar mass DM and an optimum cadence for detecting and mapping them. The lowest contour is 0.02 and the highest 0.2. The blue curve is the celestial equator. The green dot is the Large Magellanic Cloud, microlensing target for the MACHO project (Alcock et al. 1993) and others. Only Galactic stars enter the calculation as source stars; so an uptick for the LMC is absent. Compare this with the anticipated results from the LSST cadence, figure 5 of Romao et al. (2025.)